isothermal mixed boundary conditions in heat transfer, *Int. J. Heat Mass Transfer* **30,** 903–909 (1987).
3. A. T. Kirkpatrick and M. Bohn, An experimental investigation of mixed cavity natural convection in the high Rayleigh number regime, *Int. J. Heat Mass Transfer* **29,** 69–82 (1986).
4. S. Kimura and A. Bejan, Natural convection in a differentially heated corner region, *Phys. Fluids* **28,** 2980–2989 (1985).
5. R. Anderson and G. Lauriat, The horizontal natural convection boundary layer regime in a closed cavity, *Proc. 8th Int. Heat Transfer Conf.*, San Francisco, California, pp. 1453–1458 ((1986).
6. K. Torrance and J. Rockett, Numerical study of natural convection in an enclosure with localized heating from below—creeping flow to the onset of laminar instability, *J. Fluid Mech.* **36,** 33–54 (1969).
7. K. E. Torrance, L. Orloff and J. A. Rockett, Experiments on natural convection in enclosures with localized heating from below, *J. Fluid Mech.* **36,** 21–31 (1969).
8. D. Greenspan and D. Schultz, Natural convection in an enclosure with localized heating from below, *Comput. Meth. Appl. Mech. Engng* **3,** 1–10 (1974).
9. P. Chao, H. Ozoe, S. Churchill and N. Lior, Laminar natural convection in an inclined rectangular box with the lower surface half-heated and half-insulated, *J. Heat Transfer* **105,** 425–432 (1983).
10. G. Shiralkar and C. Tien, A numerical study of the effect of a vertical temperature difference imposed on a horizontal enclosure, *Numer. Heat Transfer* **5,** 185–197 (1982).
11. D. Poulikakos, Natural convection in a confined fluid filled space driven by a single vertical wall with warm and cold regions, *J. Heat Transfer* **107,** 867–876 (1985).
12. M. November, Natural convection in a rectangular enclosure heated and cooled on adjacent walls, M.S. Thesis, University of Pennsylvania, Philadelphia, Pennsylvania (1986).
13. J. D. Nicolas, Natural convection in a rectangular enclosure with partial heating of one surface, M.S. Thesis, University of Pennsylvania, Philadelphia, Pennsylvania (1991).
14 P. G. Simpkins and T. D. Dudderar, Convection in rectangular cavities with differentially heated end walls, *J. Fluid Mech.* **110,** 433–456 (1981).
15. L. Pera and B. Gebhart, Natural convection boundary layer flow over horizontal and slightly inclined surfaces, *Int. J. Heat Mass Transfer* **16,** 1131–1146 (1973).

Int. J. Heat Mass Transfer. Vol. 36, No. 16, pp. 4071–4076, 1993
Printed in Great Britain

0017 9310/93 $6.00 + 0.00

Critical heat flux in pool boiling of binary mixtures as determined by the quenching method

JYH-FUH CHEN, MING-HUEI LIU and YU-MIN YANG†

Department of Chemical Engineering, National Cheng Kung University, Tainan, Taiwan 70101, R.O.C.

(*Received* 6 *January* 1993 *and in final form* 6 *May* 1993)

INTRODUCTION

THE CRITICAL heat flux (CHF) is the highest possible nucleate boiling heat flux. For a system in which the surface heat flux is controlled, CHF is the heat flux for which there is a sudden jump in surface temperature resulting from the increase of the heat flux. For a system in which the surface temperature is controlled, CHF is the heat flux for which the surface heat flux starts to decrease as a result of an incremental change in the surface temperature. The understanding and prediction of CHF is therefore very important in the design of heat exchange equipment operating in the nucleate boiling regime. The need to understand and predict the CHF in mixtures has been driven by the ubiquitous presence of mixtures in the chemical and process industries.

A dilemma of CHF in binary mixtures is that some investigators found out for certain compositions the CHF was as much as twice the value for either pure component, but on the other hand, critical heat fluxes were found to be always between those of the pure components by different investigators. This dilemma of CHF in binary mixtures may be shown schematically by Fig. 1, which appeared originally in Collier's book [1].

As shown in Fig. 2, the bewildering status of the critical heat flux for the acetone–water binary mixture system is obvious. In this figure, $q_{c,1}$ is the ideal linear mixing law critical heat flux defined as

$$q_{c,1} = (1-x)q_{c,1} + xq_{c,2} \quad (1)$$

where $q_{c,1}$ and $q_{c,2}$ are the critical heat fluxes for pure component 1 and pure component 2, respectively, and x is the mass fraction of component 2 in the binary liquid mixture.

† Author to whom correspondence should be addressed.

It is worthy to note that the heating surfaces used by van Wijk *et al.* [2], Carne [3] and Stephen and Preußer [4] are 0.2 mm platinum wire, 3.2 mm stainless steel tube, and 14 mm nickel tube, respectively. These results revealed that the dilemma suffered seemingly because the influential roles of geometry and of geometric scale on CHF had not yet been identified or properly diagnosed.

Increased critical heat flux

The well-known effect that the CHF with small diameter wires increases with concentration of a volatile organic component to a maximum value and then decreases has been noted by van Stralen and coworkers and many other investigators. Van Stralen [5, 6] defined the CHF in terms of a bubble-packing model. Since the bubble departure diameter decreases to a minimum at the same composition as the minimum bubble growth rate, van Stralen surmised that the increase he observed in CHF was due to the higher bubble-packing density possible in the mixtures. This is an interesting coincidence, termed the 'boiling paradox', whereby the maximum CHF occurs at the minimum bubble growth rate and departure diameter. The increase in the CHF is then explained by the summation of the contributions of direct vaporization at the heated surface and the convective heat transfer caused by the bubble motion. Van Stralen showed that while the evaporation heat flux decreased with the addition of a volatile solvent to water, the convective heat flux increased by a greater margin. Thus CHF experienced an increase in the mixture in comparison to pure water.

Yang and Maa [7] explained qualitatively the maximum in CHF as being due to three intercorrelated phenomena. The first is the slowing down in bubble growth rate caused by the exhaustion of the more volatile component near the

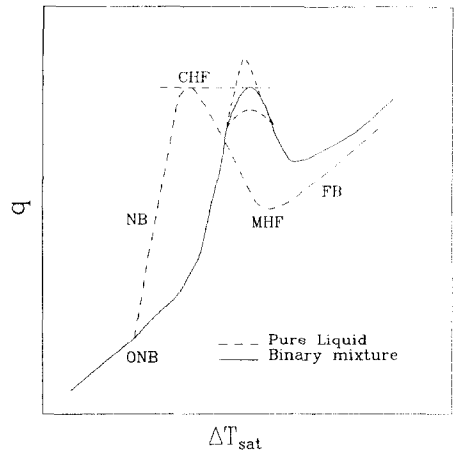

FIG. 1. Schematic diagram showing the dilemma of CHF in binary mixtures.

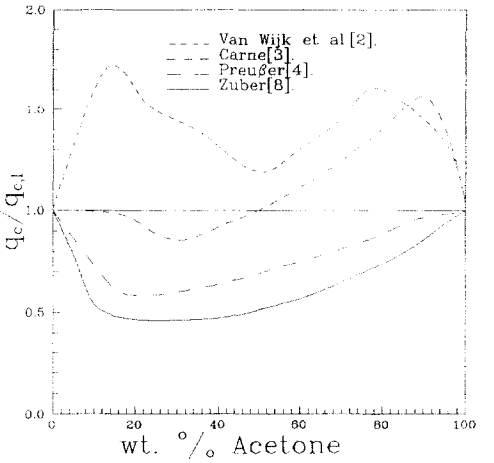

FIG. 2. Normalized pool boiling critical heat flux for acetone water mixtures. ---: 0.2 mm diameter platinum wire [2]. ——: 3.2 mm diameter stainless steel tube [3]. ———: 14 mm diameter nickel tube (as reported by Stephan and Preußer [4]).

vapor–liquid interface (the F effect), as noted by van Stralen. The second is the retardation of bubble coalescence due to surface tension gradient caused by evaporation of the component of lower surface tension (the M effect). The third is the retardation of bubble coalescence due to surface tension gradient caused by the fast stretching of the vapor liquid interface (the Y effect).

The influence of the mass diffusion effect can be expressed by a function

$$F = (x-y)\left(\frac{\alpha}{D}\right)^{0.5}\left(\frac{C_p}{h_{fg}}\right)\left(\frac{dT}{dx}\right) \tag{2}$$

in which x, y are the mass fraction in liquid and vapor phase, respectively; α, D, C_p, h_{fg} are the thermal diffusivity, mass diffusivity, liquid specific heat and latent heat of vaporization, respectively; and T is the saturation temperature of a liquid. Since $(x-y)$ and (dT/dx) are always of the same sign, the value of F in equation (2) is always positive. That is, the bubble growth rate in the binary mixture is always slower than that of an equivalent pure fluid with the same physical properties as the mixture except when $y = x$. The F values usually have a maximum at a specific concentration for each mixture. It has two maxima for the cases of azeotropic mixtures.

A surface tension gradient along the vapor–liquid interfaces between neighboring bubbles may be built up due to a concentration gradient caused by evaporation. The flow of the liquid as a consequence of a surface tension gradient along a vapor–liquid interface is known as the Marangoni effect. In the so-called positive binary system, the more volatile component has the lower surface tension. The more volatile component in the thin liquid layer between two adjacent vapor bubbles is exhausted; therefore, the local value of the surface tension is higher there than that of the rest of the bubble wall. The walls of both bubbles contract in the vicinity of the original tangent plane, and the coalescence is therefore avoided. The influence of the surface tension gradient can be measured by a function

$$M = (x-y)(d\sigma/dx). \tag{3}$$

This equation indicates that the resistance to coalescence depends on the sign of $d\sigma/dx$, the surface tension gradient with respect to composition. In the positive binary systems, $d\sigma/dx$ is negative and M is positive. On the other hand, in the negative binary systems, M is negative.

In multicomponent systems extension of an interface causes an increase in interfacial tension, and a contraction causes a decrease. This dynamic surface effect, which is the conjugate of the Marangoni effect noted above, is a result of slowness of migration of the molecules of lower surface tension from the bulk to the adsorption layer at the interface or vice versa. This effect bestows the elasticity on a thin liquid film between two adjacent vapor bubbles, and the coalescence of bubbles is therefore inhibited. The influence of the dynamic surface effect can be expressed by a function

$$Y \equiv \theta(x)\left(\frac{d\sigma}{dx}\right)^2 \tag{4}$$

where

$$\theta(x) = \frac{x(1-x)}{1-x+kx} \tag{5}$$

in which k is the ratio of molar volumes of the low surface tension component to that of high surface tension component. The value of Y is proportional to the local surface tension rise of a binary liquid due to stretching of certain rate and thus is a quantitative measurement of the dynamic surface effect. In the boiling of a liquid mixture, the growth and coalescence of vapor bubbles are dynamic processes and the stretching of vapor–liquid interface is intensively involved. Close relationship between the behaviors of these processes (and consequently the process of boiling heat transfer) and the Y value is therefore expectable.

Reduced critical heat flux

In contrast to the case when boiling occurs along a thin wire, however, different results were obtained when boiling occurs on a horizontal tube with diameter several magnitudes larger than the departure diameter of a single bubble. Critical heat fluxes were found to always vary between those of the pure components. The variation of CHF with composition is qualitatively well described by the equation of Zuber [8] based on hydrodynamic instability model for pure liquids on flat-plate heaters:

$$q_{c,Zuber} = \frac{\pi}{24}\rho_g^{1/2}h_{fg}[\sigma g(\rho_f-\rho_g)]^{1/4} \tag{6}$$

in which ρ_g and ρ_f are saturated vapor and liquid density, respectively, and g is gravitational acceleration.

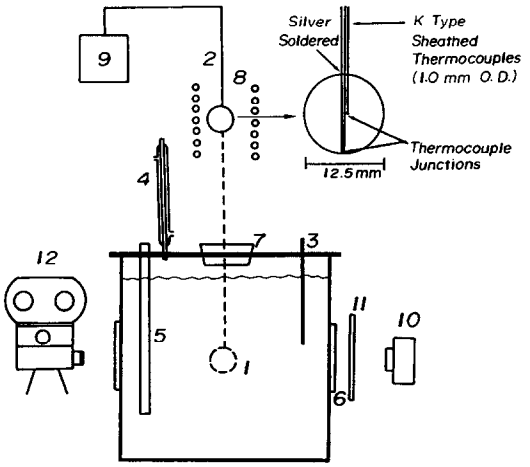

FIG. 3. Schematic diagram of the quenching apparatus. 1. Test sphere. 2. Thermocouples and support stem. 3. Thermometer. 4. Reflux condenser. 5. Supplementary heater. 6. View windows. 7. Silicone rubber plug. 8. Induction heating coil. 9. Data acquisition system. 10. Light source. 11. Diffuser. 12. Camera or high-speed camera.

No general model or predictive method can currently explain the seemingly conflicting experimental results.

The objective of this work is to provide the original measurements of the pool boiling CHF in saturated *n*-propanol (normal propyl alcohol, NPA)–water binary mixtures over the entire range of compositions on a quenching sphere of 12.5 mm diameter, which begins to approximate industrial-size elements. This binary system is of particular interest because it has an azeotrope at 0.717 mass fraction (or 0.432 mole fraction) of *n*-propanol and hence is suitable for simultaneous investigation of the mass diffusion effect (the *F* effect), the Marangoni effect (the *M* effect), and the dynamic surface effect (the *Y* effect) on CHF if these effects exist.

EXPERIMENTAL

The use of quenching techniques to determine boiling curves has been proved to be a more rapid and easier method than traditional steady-state methods. However, the boiling curve from a quenching test depends on the dimensions of the quenching solid, its material of construction, the dimensions of the enclosing vessel, and sometimes the location of the thermocouple used to get the time vs temperature data. These factors can be standardized so that the resulting data are applicable to commercial equipment [9]. The quenching apparatus used in this work was designed mainly according to their suggestions.

Figure 3 shows the schematic diagram of the quenching apparatus and the copper test sphere of 12.5 mm diameter with two K-type sheathed thermocouples silver-soldered at the center and near the surface. The surface of the sphere was carefully polished with fine sandpaper, cleaned, and electroplated with chromium. Two liters of liquid were contained in a 14 cm I.D. stainless steel tank. The tank was insulated but some heat loss was noticeable. A supplementary heater was installed for the purposes of bringing up the temperature of the liquid pool at the beginning of the experiment and maintaining it at the boiling point of the test liquid. The pool temperature was measured by a calibrated thermometer. A reflux condenser was provided for condensing the vapor generated in the pool. Boiling on the sphere can be illuminated, observed, and photographed through view windows on the front and rear side of the tank.

The test sphere was induction heated in a high frequency coil to about 560°C. When a uniform temperature was reached, the data acquisition process was started and then the sphere was plunged into the saturated liquid pool with 6 cm depth of immersion by removing the silicone rubber plug and lowering the support stem. Data acquisition was started about 1 s before quenching. In order to avoid any possible electrical noise, power supplies to induction and supplementary heaters were shut off just before starting data acquisition. No significant subcooling or boil-off was noticed during quenching experiment.

The signal from thermocouples was amplified and fed to the interfaced personal computer through analog-to-digital converter. The sampling time was adjusted to 5 ms and the sampling always lasted for 64 s in this work.

Pure water, pure *n*-propanol, and ten of their mixtures—including 5, 10, 20, 45, 69, 71.7, 72, 74, 80 and 90 wt% *n*-propanol—were studied. It should be noted that the mixture at azeotropic composition of 71.7 wt% *n*-propanol was also included.

DATA REDUCTION AND ANALYSIS

In a quenching experiment, the record is that of time vs temperature at known locations inside the solid being quenched. What is desired is the heat flux at the surface of the solid vs the temperature driving force for boiling (surface temperature minus liquid temperature). This estimation of the surface heat flux from interior temperature measurements is called the inverse heat conduction problem (IHCP).

The mathematical model describing the IHCP for the estimation of the surface heat flux is given below. During quenching experiments, the surface of the sphere is exposed to an external time-dependent boundary condition starting at time $t = 0$. The temperature distribution inside the sphere upon quenching is described by the one-dimensional transient heat conduction equation:

$$\frac{\partial T}{\partial t} = \alpha(T)\left(\frac{\partial^2 T}{\partial r^2} + \frac{2}{r}\frac{\partial T}{\partial r}\right), \quad 0 \leqslant r < R, \quad t > 0 \tag{7}$$

with the boundary and initial conditions:

$$T = T_0, \quad t = 0, \quad 0 \leqslant r \leqslant R \tag{8}$$

$$\frac{\partial T}{\partial r} = 0, \quad r = 0, \quad t > 0 \tag{9}$$

$$T = f(t), \quad r = R, \quad t > 0 \tag{10}$$

where T_0 is the initial uniform temperature of the sphere and $f(t)$ is the experimentally measured surface temperature history. R is the sphere radius.

Finite difference procedure posed in spherical coordinates was used. Detailed derivation of Crank–Nicolson equations is given elsewhere [10]. The resulting tridiagonal matrix is then solved by Gaussian elimination. Variable thermal properties are included in the procedure. The surface heat flux from the sphere can then be determined by the calculated temperature profile through Fourier's first law of heat conduction. The numerical solution of the problem and the surface heat flux calculation were implemented on a personal computer.

EXPERIMENTAL RESULTS AND DISCUSSIONS

The model given by equations (7)–(10) has been shown to adequately describe the problem and the numerical solution was found to be quite accurate, by comparing the calculated and experimentally measured temperatures at the center of the sphere during quenching in saturated pure water [10, 11].

Figure 4 shows the general trend of concentration effect, over the entire range of compositions, on boiling heat transfer with 12 quenching curves. Conventional boiling curves can be easily obtained and critical heat fluxes were determined from boiling curves as the peak heat fluxes. Five to

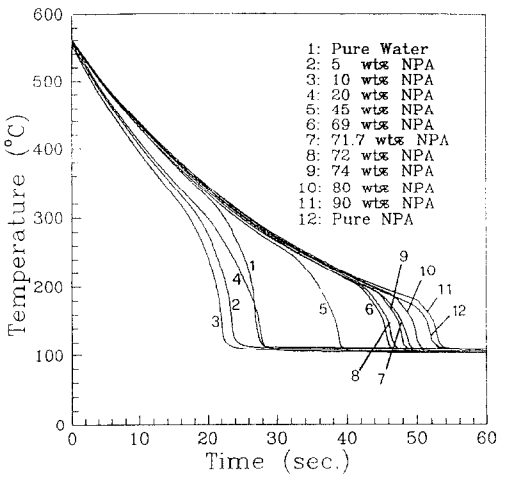

FIG. 4. Quenching curves (surface temperature vs time) for pure water, pure *n*-propanol, and ten of their mixtures.

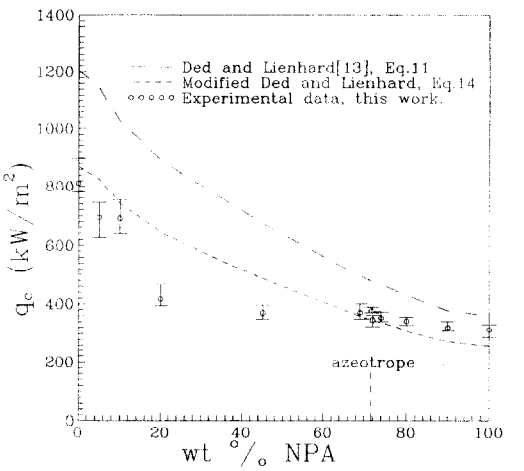

FIG. 5. Variation of critical heat flux with composition for *n*-propanol–water binary system.

nine runs have been conducted for each composition, and the average and standard deviation of CHF data are shown in Table 1. The experimental data reveal that the critical heat fluxes of *n*-propanol–water binary mixtures are always between those of pure water and pure *n*-propanol. This trend can more clearly be seen by showing the data in Fig. 5. The symbol, upper bar, and lower bar in Fig. 5 represent the average, highest, and lowest CHF values, respectively, for a particular composition of binary mixture.

The appearance of bubbles in the boiling of binary mixture is considerably different from that of pure water. *n*-Propanol causes more, smaller vapor bubbles on the surface, especially in transition and nucleate boiling regimes.

Figure 6(a) shows a comparison of the results of this work and two other independent studies on the CHF for *n*-propanol–water system. The bewildering status of CHF similar to that in acetone–water mixtures, as shown in Fig. 2, showed itself again in *n*-propanol–water mixtures. These experimental results of CHF in binary systems give strong evidence of the influential effects exerted by geometry and geometric scale.

Figure 6(b) shows the variation of the values of F, M and Y with composition for *n*-propanol–water system [12]. All curves in this figure show distinct maximum at certain relatively low concentration of *n*-propanol. Another maximum of the F curve occurs at the concentration above azeotropic point. M-value is negative when the mixture forms a negative binary system, thus opposite effect to that exhibited in positive binary system is expected. On the other hand, the Y curve has only one peak. It is worth noting that van Wijk *et al.* explained the maximum in their CHF data as being due to the F effect. Of course, it is doubtful that the models used for deriving F, M and Y may not correspond exactly to the actual various experimental conditions, so that exact quantitative agreement would be unexpected. However, if F, M and Y effects are important for binary mixtures, they should affect the phenomena of bubble growth and coalescence for bubbles on a thin wire as well as for bubbles on a larger surface. The trend of the effect is more significant than the specific values.

While the F, M and Y effects may be prevailing as indicated by the appearance of bubbles in the boiling of binary mixtures, the experimental results of this work, however, revealed that the CHF cannot be explained by the F, M and Y effects for *n*-propanol–water mixtures on a sphere of 12.5 mm diameter. The case is also true for acetone–water mixtures on a tube of 14.4 mm O.D. Although the phenomenon is not clearly understood, it appears that the extent of the contribution from convective heat transfer caused by the bubble motion may be very different to that on a thin wire or on a larger surface with different geometry. This may result in the fact that the CHF in boiling of binary mixtures may be increased or reduced as shown in Fig. 1. Nevertheless, minima have been obtained for thin wires and large heating

Table 1. Comparison between experimental and predicted CHF data (kW m^{-2})

wt. % of *n*-propanol (liquid)	Experimental Average	CHF Standard Deviation	Ded and Lienhard CHF, equation (11)	Error (%)	Modified Ded and Lienhard CHF, equation (14)	Error (%)
0	812	35	1206	49	871	8
5	694	41	1145	65	827	20
10	691	36	1027	49	742	8
20	416	28	893	114	644	55
45	370	20	674	82	487	32
69	371	17	498	34	359	−3
71.7	378	6	480	27	347	−8
72	347	13	478	38	345	0
74	353	12	469	33	338	−4
80	343	9	430	25	310	−9
90	320	7	378	18	273	−14
100	314	11	360	15	260	−17
			Average error = 46%			15%

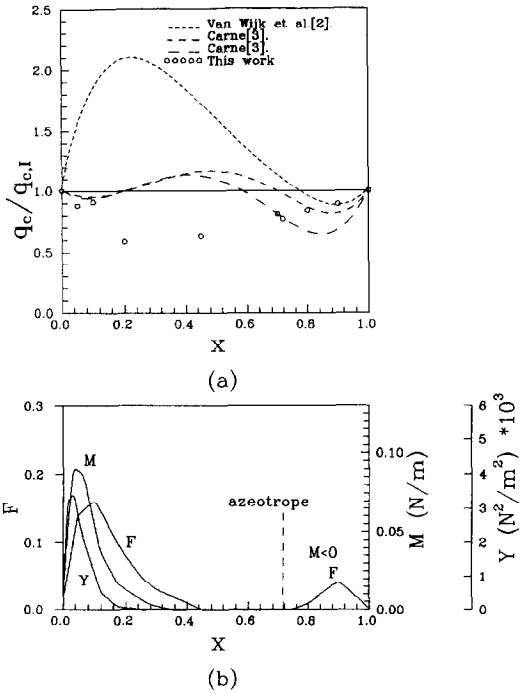

FIG. 6. (a) Normalized pool boiling critical heat flux for *n*-propanol–water binary mixtures. ---: 0.2 mm diameter platinum wire [2]. – – –: 1.6 mm diameter stainless steel tube [3]. ———: 3.2 mm diameter stainless steel tube [3]. ○○○: 12.5 mm diameter copper sphere (this work). (b) *F*, *M* and *Y* as functions of composition for *n*-propanol–water binary mixtures [12].

surfaces have also been found to result in a maximum in CHF rather than in a minimum. Further systematic studies of parametric effects on CHF of binary mixtures are much desirable.

Ded and Lienhard [13] formulated a hydrodynamic prediction for pool boiling critical heat flux of pure liquids on sphere:

$$\frac{q_c}{q_{c,Zuber}} = \frac{1.734}{\sqrt{R'}}, \quad 0.1 \leqslant R' \leqslant 4.26 \tag{11}$$

and

$$\frac{q_c}{q_{c,Zuber}} = 0.84, \quad R' \geqslant 4.26 \tag{12}$$

where $q_{c,Zuber}$ is the critical heat flux given by equation (6) and R' is a dimensionless radius, the Laplace number, defined by

$$R' = R\left[\frac{g(\rho_f - \rho_g)}{\sigma}\right]^{1/2} \tag{13}$$

where R is the radius of the sphere.

The dimensionless radii, R', are 2.49 and 4.03 for pure water and pure *n*-propanol, respectively. For binary mixtures studied in this work, the dimensionless radii have also been calculated by evaluating the relevant physical properties [11].

With the postulation that Ded and Lienhard's formulations can also apply to mixtures, CHF values are predicted by using equation (11), and are shown in Table 1 with an average error of 46%. It is evident that Ded and Lienhard's correlation qualitatively describe but overpredict CHF values of this binary system. Also shown in Table 1 are the predicted CHF values, with an average error of 15%, by a modified correlation of Ded and Lienhard's prediction

$$\frac{q_c}{q_{c,Zuber}} = \frac{1.257}{\sqrt{R'}}, \quad 2.49 \leqslant R' \leqslant 4.03 \tag{14}$$

in which the value of the constant was obtained by adjusting it to give a minimum average error based on the compositions studied in this work. The comparison between experimental CHF data and those predicted by equations (11) and (14) is also shown in Fig. 5.

Although the modified correlation of Ded and Lienhard's prediction, equation (14), is found to reasonably describe the experimental results of this work, making an attempt to provide scientific explanation for the fitted constant value of 1.257 seems to be impossible before more experimental studies of parametric effects on CHF of binary mixtures can be documented. At the same time, it is not at all clear what the effects of mass diffusion and/or other surface processes will be on the formation of vapor jets and their stability, which are essential to the hydrodynamic instability model for predicting CHF.

CONCLUSIONS

Pool boiling critical heat flux values for pure water, pure *n*-propanol, and ten of their mixtures including the azeotrope were measured by the quenching method. The experimental results show that the critical heat flux of a binary mixture is between those of pure water and pure *n*-propanol, and is a nonlinear function of composition. It revealed that while the mass diffusion effect (the *F* effect), the Marangoni effect (the *M* effect), and the dynamic surface effect (the *Y* effect) may be prevailing as indicated by the appearance of bubbles in the boiling of binary mixtures, they play a minor role in CHF phenomenon.

By taking into account the variation of relevant physical properties with composition, Ded and Lienhard's correlation, equation (11), is found to qualitatively describe but overpredict the experimental results of this binary system within the size range $2.94 \leqslant R' \leqslant 4.03$. The closeness of the prediction can be improved by adjusting the value of the constant in equation (11).

Although the phenomenon is not clearly understood, the bewildering status of CHF in binary mixtures is due to the extent of the contribution from convective heat transfer caused by the bubble motion on different boiling surface of different geometry and geometric scale.

Acknowledgement—This study was supported by the National Science Council of the Republic of China through grant No. NSC 81-0402-E006-01. Professor Jer Ru Maa is gratefully acknowledged for his helpful discussions.

REFERENCES

1. J. G. Collier, *Convective Boiling and Condensation* (2nd Edn), p. 406. McGraw-Hill, New York (1981).
2. W. R. van Wijk, A. S. Vos and S. J. D. van Stralen, Heat transfer to boiling binary liquid mixtures, *Chem. Engng Sci.* **5**, 68–80 (1956).
3. M. Carne, Some effects of test section geometry in saturated pool boiling on the critical heat flux for some organic liquids and liquid mixtures, *CEP Symp. Ser., No. 59* **61**, 281–289 (1965).
4. K. Stephan and P. Preußer, Heat transfer and critical heat flux in pool boiling of binary and ternary mixtures, *Ger. Chem. Engng* **2**, 161–169 (1979).
5. S. J. D. van Stralen, The mechanism of nucleate boiling in pure liquids and in binary mixtures—Part I, *Int. J. Heat Mass Transfer* **9**, 995–1020 (1966).
6. S. J. D. van Stralen, The mechanism of nucleate boiling in pure liquids and in binary mixtures—Part II, *Int. J. Heat Mass Transfer* **9**, 1021–1046 (1966).

7. Y. M. Yang and J. R. Maa, Dynamic surface effect on the boiling of mixtures, *Chem. Engng Commun.* **25**, 47–62 (1984).
8. N. Zuber, On the stability of boiling heat transfer, *Trans. ASME* **80**, 711–720 (1958).
9. J. W. Westwater, J. J. Hwalek and M. E. Irving, Suggested standard method for obtaining boiling curves by quenching, *I&EC Fundam.* **25**, 685–692 (1986).
10. H. S. Lin, Studies on pool boiling heat transfer by quenching with sphere, M.S. Thesis, Chem. Engng Dept., National Cheng Kung University, Tainan, Taiwan (1990).
11. J. F. Chen, Studies on pool boiling heat transfer of binary mixtures by quenching with sphere, M.S. Thesis, Chem. Engng Dept., National Cheng Kung University, Tainan, Taiwan (1992).
12. Y. L. Tzan and Y. M. Yang, Pool boiling of binary mixtures, *Chem. Engng Commun.* **66**, 71–82 (1988).
13. J. S. Ded and J. H. Lienhard, The peak pool boiling heat flux from a sphere, *A.I.Ch.E. Jl* **18**, 337–342 (1972).

Int. J. Heat Mass Transfer. Vol. 36, No. 16, pp. 4076–4078, 1993
Printed in Great Britain

0017-9310/93 $6.00 + 0.00

Dryout under oscillatory flow condition in vertical and horizontal tubes—experiments at low velocity and pressure conditions

MAMORU OZAWA and HISASHI UMEKAWA
Department of Mechanical Engineering, Kansai University, Yamate-cho 3-3-35, Suita, Osaka 564, Japan

YOHJI YOSHIOKA
Kubota Ltd., Shikitsu-higashi, Naniwa, Osaka 556-91, Japan

and

AKIO TOMIYAMA
Department of Mechanical Engineering, Kobe University, Nada, Kobe 657, Japan

(*Received* 24 *December* 1992 *and in final form* 27 *April* 1993)

1. INTRODUCTION

DENSITY wave oscillation in boiling channels induces a drastic reduction of the critical heat flux (CHF) from the value under stable operating conditions [1, 2]. The increase in the amplitude of the oscillation may enhance the initiation of the premature dryout, and the decrease in the period of oscillation may enhance the rapid cooling and/or rewetting after the premature dryout. The CHF problems under flow oscillations should be analyzed taking account of the effects of these two factors. The period and the amplitude of the density wave oscillation are closely related to each other and are strong functions of the operating conditions, such as a mass flux and a heat flux, as well as a system configuration. One of the approaches to provide the fundamental understanding of the phenomena is to conduct the CHF experiment imposing a forced flow oscillation with a predetermined period and amplitude on a mean flow. Although such approach has been conducted almost 30 years ago by Sato *et al.* [3] and Ishigai *et al.* [4], sufficient understanding has not been obtained so far owing to the limitations of the experimental range. Thus systematic experiments have been conducted to verify the effects of the amplitude and the period of the flow oscillation on the CHF using vertical and horizontal boiling channels, and experimental data of the CHF with the forced flow oscillation are presented in this report.

2. EXPERIMENT

The main parts of the test loop are a reserve tank of ion-exchanged water, a gear pump, a calming section, a test section, a separator, and a flow oscillator as shown in Fig. 1. The water in the reserve tank was degassed by boiling prior to the experiments. The test section was a SUS304 tube of the dimension 5.0 mm I.D., 6.0 mm O.D. and 900 mm in length, and was heated by Joule heating of the A.C. power. The steam–water separator was opened to the atmosphere and thus all the experiments were conducted at the atmospheric pressure. The tube wall temperatures were measured using C-A thermocouples of 0.1 mm diameter at every 50 mm location along the test section. The pressure drops at the calming section and the test section were measured with D.P. cells. The pressure drop in the calming section was used for monitoring the flow oscillation.

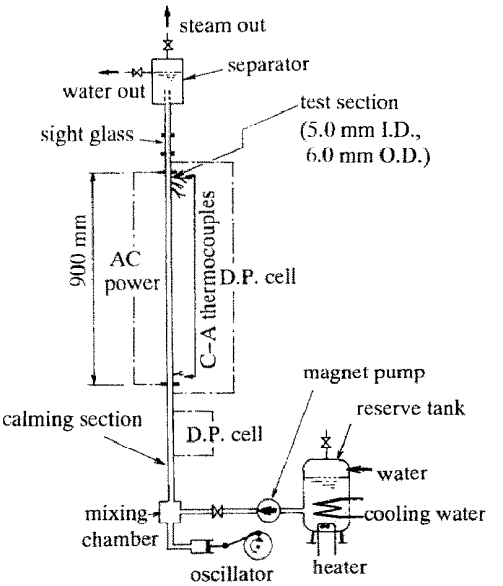

FIG. 1. Experimental apparatus.